

Strain management in HTS high current cables

N. Bykovsky, D. Uglietti, R. Wesche, and P. Bruzzone

Abstract—The best performing HTS conductors are available in the form of thin tapes with operating current in the range of 200 A at the operating conditions. To realize conductors with high current carrying capability, in the range of several tens kA, a large number of tapes must be assembled in a cable. The conventional stranding methods for round conductors are not applicable to thin tapes. CRPP has developed an assembly concept based on twisted stacks of tapes soldered into a copper profile. The ability to withstand bending and torsion strain is the main issue for the design of a high current flat cable based on twisted stacks of HTS tapes. An analytical mechanical model was developed and validated with the results of measurements. Parametric analyses are used to select the optimum layout for the first full size prototype of the coming HTS conductor for fusion. Various configurations of the cable are presented and compared, paying attention in particular to the strain acting in the tape. The chosen set of cable parameters satisfies electromechanical limitations and provides feasibility of strands winding.

Index Terms—HTS tapes, strains, high current cable

I. INTRODUCTION

NEXT FUSION PROJECT - DEMO – triggered new activity in high current cables engineering. Both LTS and HTS cable’s solutions are considered in the labs and nowadays using HTS tapes for such purposes looks quite promising because of high temperature margin, exceptional access to field range >23 T (limit for LTS application) and coming tape’s price collapse, pledged by its manufacturers. There are several main specific requirements for future fusion’s cables:

- Current >60 kA at field >12 T.
- Engineering current density >50 A/mm²
- Stability under high pressure due to Lorentz force
- Copper cross-section >500 mm² (for protection)

According to the approach of CRPP to build a high current, force flow conductor starting from thin tape [1], a stack of tapes is encased between two half round copper profiles and twisted, see Fig. 1. This assembly is called “strand”. The number of strands to be assembled in a cable, e.g. a cored flat cable, depends on the conductor requirement. The modularity of this approach represents a progress compared to the twisted-stack conductor proposed by MIT [2].

The main parameters of the strand are: D – diameter of the strand, t, w – thickness and width of the slot, n – number of tapes, h – twist-pitch of the strand (length over which twist

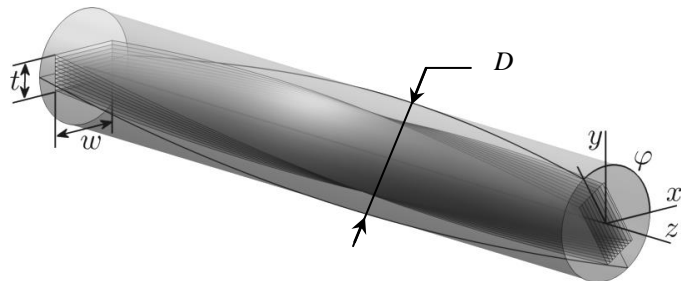


Fig. 1. Sketch of the strand.

angle ϕ changes in 360°). Depending on sequence, there are two ways of strand manufacturing: *first-twisted-then-soldered* (TS) and *first-soldered-then-twisted* (ST). TS allows to avoid strain accumulation effects in the stack, which actually happened in ST, and to use twist-pitch h in range of few hundreds mm without degradation of tapes performance.

The first bending trials of the strand showed poor ability to withstand mechanical loads with early cracks propagation between copper profiles and stack delamination [1]. Hence, there are two objectives of this work: the first is to optimize copper profiles with aim to improve strand bending properties (section II) and the second is to find suitable cable design for the full size prototype with respect to the fusion cables requirements and electromechanical limits (section III, IV).

II. BENDING OF THE STRAND

Four samples were prepared in TS sequence for the bending test with the twist-pitch $h = 300$ mm and number of HTS tapes $n = 15$ – SuperPower SCS4050 4 mm width tapes with $I_c(77K, sf) \approx 78$ A. Two factors were studied during the profile optimization – preliminary profile annealing (1 hour at 300° C), which makes the material softer, and geometry modification of the cross-section. Cracks between copper profiles and delamination of the stack begin under appropriate critical bending radii, which are given in the Table I together with the summary of the sample properties.

The prediction of strand I_c is based on the electromagnetic

Table I. Sample properties

Sample name	Non-heated	Normal	Plus	S
Cross-section				
Diameter, mm	6.2	6.2	7.0	7.0
Length, cm	100	100	50	50
Expected $I_c(77K, sf)$, A	890	870	870	880
Measured $I_c(77K, sf)$, A	915	885	870	890
Preliminary profile annealing	No	Yes	Yes	Yes
R, mm (cracks)	500	240	<150	<150
R, mm (delamination)	400	<150	<150	<150

Manuscript received July 31, 2014.

model of the stack of HTS tapes [3]. The prediction is in good agreement with the results, within 3%, which means absence of degradation during the TS manufacturing stage.

Great influence of the preliminary profile annealing was observed (see Table I: ‘Non-heated’ vs ‘Normal’). Cracks between profiles and delamination of the stack in ‘Non-heated’ sample begin at bending radii 500 mm and 400 mm [1] in contrast with other samples, which are much more stable to the bending loads.

New geometries of strand’s cross-sections are presented by ‘Plus’ and ‘S’ samples (see Table I and Fig. 2). Actually, these samples again have improved bending properties, but higher diameter (lower current density) and more complicated production of the ‘S’ profiles make them less attractive.



Fig. 2. The copper profiles of the ‘S’ (left) and ‘Plus’ (right) strands.

The behavior of the critical current under the bending load was studied in both analytical and experimental ways. The exact analytical position of the stack of tapes with pure circle form of the center-line is expressed by the system of coordinates (1).

$$\sigma(s,u,v) = \begin{cases} x = \left(R - u \cos\left(\frac{2\pi}{h}s\right) + v \sin\left(\frac{2\pi}{h}s\right) \right) \cdot \cos\frac{s}{R} \\ y = \left(R - u \cos\left(\frac{2\pi}{h}s\right) + v \sin\left(\frac{2\pi}{h}s\right) \right) \cdot \sin\frac{s}{R} \\ z = u \sin\left(\frac{2\pi}{h}s\right) + v \cos\left(\frac{2\pi}{h}s\right) \end{cases} \quad (1)$$

(u, v) – coordinates of the stack’s cross-section: $-w/2 \leq u \leq w/2$, $-t/2 \leq v \leq t/2$; s – the arc length of the center-line (natural parameterization) $\gamma(s) = \sigma(s, 0, 0)$; R – bending radius. Visualization of (1) is given in Fig. 2.

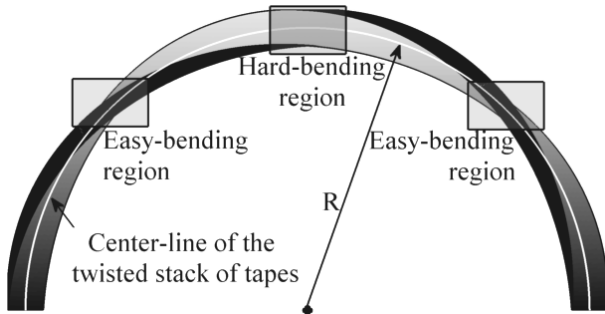


Fig. 2. Bent twisted stack of tapes

Depending on the stack orientation, there are two definitions for regions along the sample length – *easy-bending region* (EB), where the tapes’ face is perpendicular to the bending plane, and *hard-bending region* (HB), where the tapes’ face is in the bending plane.

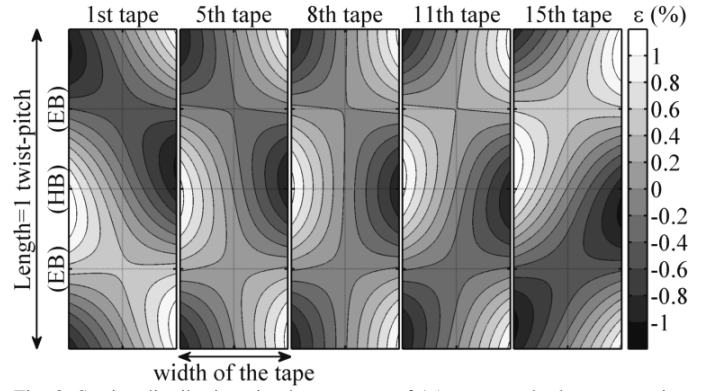


Fig. 3. Strains distributions in chosen tapes of 15-tapes stack along one twist-pitch length and width of tape at $h = 300$ mm, $R = 200$ mm.

The acting axial strains can be easily found through its definition: $\varepsilon = (dl - ds) / ds$, $dl = \sqrt{dx^2 + dy^2 + dz^2}$. As long as the TS approach is used, one should also take into account “sliding” effects in the stack at the twisting stage by adding the relaxation strains ε_0 [2, 4]. This effect leads to zero axial force in each tape’s cross-section of the straight twisted stack. Assuming $h, R \gg t, w$, total axial strains may be simplified to the following form:

$$\varepsilon_{total} = \frac{1}{2} \left(\frac{2\pi}{h} \right)^2 \left(u^2 - \frac{w^2}{12} \right) + \frac{u \cos\left(\frac{2\pi}{h}s\right) - v \sin\left(\frac{2\pi}{h}s\right)}{R} \quad (2)$$

Equation (2) has a simple structure: the first term expresses pure twisting and the second – pure bending. Limit cases of $h = \infty$ or $R = \infty$ gives the well-known results for bent non-twisted or straight twisted tapes. The total strains (2) in the five chosen tapes of 15-tapes stack at twist-pitch $h = 300$ mm and bending radius $R = 200$ mm are given in Fig. 3.

In order to obtain the critical current of the strand at given bending radius from the strains distribution, one should use appropriate $j_c(\varepsilon)$ dependence of the tape. In case of SuperPower SCS4050 tape the appropriate expression was found in [2]. The last step is to solve the problems of parallel (along the stack cross-section) and serial (along the tape length) connection of superconducting regions. The serial part of the problem also requires known values of n parameter, which have been evaluated with $n = n_0^{j_c / j_{c0}}$, $n_0 = 25$.

Comparison between the analytical model and results of the measurements of 4 samples is plotted in Fig. 4. Measurements

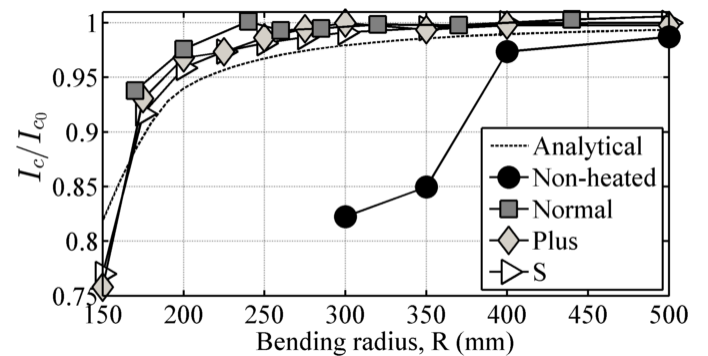


Fig. 4. Strand’s critical current (77K, sf) as a function of bending radius.

were carried out at 77 K and in self-field of the strand. The very important fact of YBCO HTS tapes is that critical current dependence over strains is even weaker at 4.2 K and in the broad range of magnetic fields 2-14 T [5]. It allows considering the results in Fig. 4 as over-conservative.

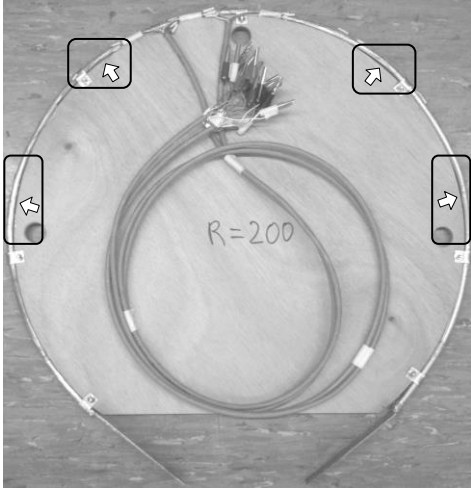


Fig. 5. Bent strand: HB regions are highlighted with boxes.

Deviations between calculation and measurements may be explained by the real form of the strand center-line. In contrast with the model assumption of pure circle form, the local bending radius of HB is higher than for EB (Fig. 5) as long as the HB regions are stiffer than EB [6]. Since EB is quite tolerant to the bending, higher I_c is obtained.

The parameters of the “normal” sample (see Table I) were chosen for the following optimization of the cable design and for the future strands of the first full-size prototype.

III. CABLE DESIGN OPTIMIZATION

The selected copper cored Rutherford design (Fig. 6) allows producing fully transposed, flat cable with high current density [7]. The edges of the cable are strain sensitive regions.

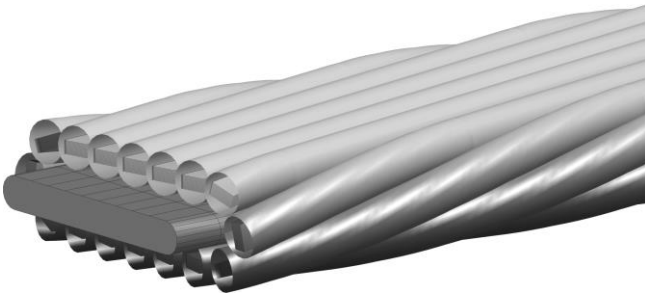


Fig. 6. Cored Rutherford cable design.

In order to optimize the cable design, the following target requirements should be fulfilled:

- Number of strands $N > 16$
- Strand bending radius $R < 240$ mm
- Cable twist-pitch $L < 1.1$ m

Depending on the core thickness g and the width of the flat part f (function of N, g, D), three cable configurations with CRPP strands are presented in Fig. 7.

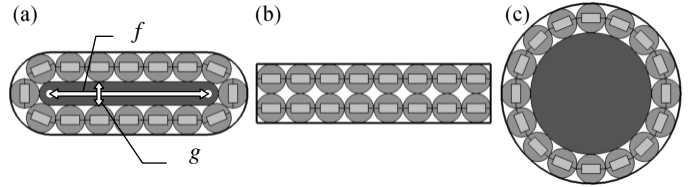


Fig. 7. Cable configurations: (a) “general” (arbitrary g), (b) “flat” ($g = 0$), (c) “circle” ($f = 0$).

The set of four cable parameters – (g, L, N, R) – has to be optimized. The first optimization step is to find appropriate core dimensions and the fast way to do this is to analyze the curvature of the strand center-line at the cable edge. The position of the center-line $\gamma(s)$ is described by a helix line with winding angle θ and radius $r = (g + D)/2$:

$$\gamma(s) = \left\{ r \cos \frac{s \sin \theta}{r}, r \sin \frac{s \sin \theta}{r}, s \cos \theta \right\} \quad (3)$$

where s – the arc length of the line. In case of natural parameterization, the expression for curvature has the simplest form [8]: $k = 1/R = |\dot{\gamma}(s)| = \sin^2 \theta / r$, and in terms of cable parameters, the bending radius is written as:

$$R = \frac{g + D}{2 \sin^2 \theta} \quad (4)$$

The expression for the twist-pitch of the cable is another term to link the cable parameters:

$$L = (2f + \pi(g + D)) \cdot \cot \theta \quad (5)$$

The peak strain can be simply obtained by $\varepsilon = d/R$, where d is the distance from the center-line to the point of interest. Taking into account $\theta \ll 1$, the peak strains for (b) and (c) cable configurations as functions of the cable twist-pitch are given below:

$$\begin{aligned} \varepsilon_{flat} &\approx \frac{2dD(N+1)^2}{L^2} \\ \varepsilon_{circle} &\approx \frac{2\pi dDN}{L^2} \end{aligned} \quad (6)$$

A comparison between the cable configurations in Fig. 8 for $N = 20$ strands and $d = 2$ mm confirms the anticipated result – with changing core thickness g one may control the peak strain in the cable between two limit cases: “flat” and “circle”. With increasing g the strain in the cable decreases, but the current density and the cable tolerance to bending will also

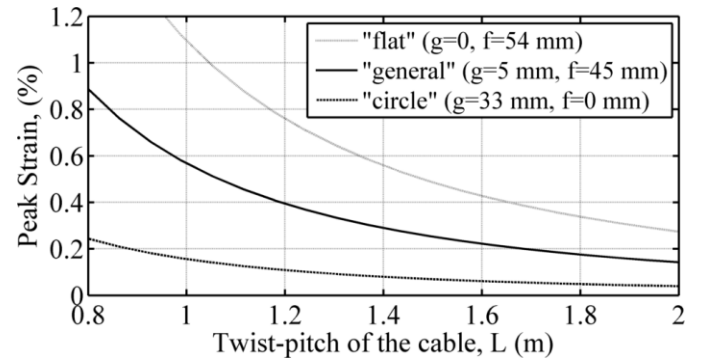


Fig. 8. Comparison of 20-strands cable configurations in terms of peak strain.

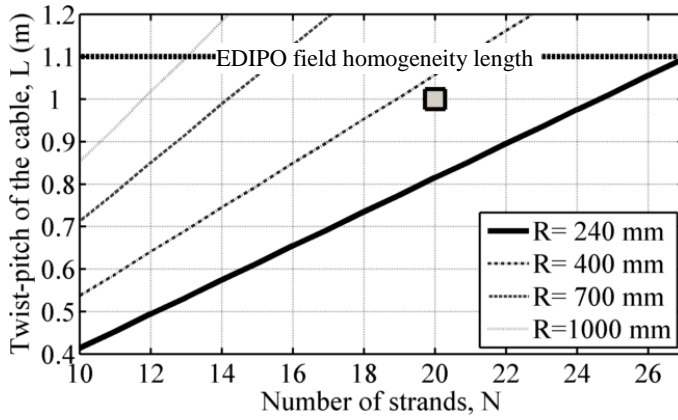


Fig. 9. Design map for the cored Rutherford cable with CRPP strands for core thickness $g = 5$ mm.

decrease and vice versa. In such conditions, $g = 5$ mm is chosen as the compromise for the full size prototype.

Fixed core thickness and strand diameter allow varying the two left parameters of the cable – twist-pitch L and number of strands N in order to obtain the contour plot of the bending radius R for each cable configuration. This design map of the cable with core thickness $g = 5$ mm is presented in Fig. 9.

The chosen parameters for the full size prototype are highlighted with square mark in Fig. 9. The full set of cable parameters is given in Table II and this set fulfills the design requirements for the cable.

Table II. Parameters of the cable

Level	Parameter	Value
Tape	thickness of tape (mm)	0.1
	width of tape, w (mm)	4
	number of tapes, n	16
Strand	twist-pitch of the strand, h (mm)	320
	diameter of the strand, D (mm)	6.2
	number of strands, N	20
Cable	twist-pitch of the cable, L (mm)	1000
	thickness of core, g (mm)	5

With this set of the parameters, the 60 kA class cable with 700 mm² cross-section of the copper and 54 A/mm² engineering current density is expected.

The performance of the full size prototype will be tested in the new EDIPO test facility at CRPP [9].

IV. STRAND WINDING ON THE CORE

Before the construction of the whole cable, a test to verify set of the cable parameters from Table II was carried out. Strand with “normal” layout from Table I is prepared for test. The 5 mm thick aluminum core allows winding the strand with angles corresponding to the cable pitches from 2 m down to 0.8 m with 0.2 m step, Fig. 10 (a). The most sensitive orientation of the strand – HB on the cable edge – is chosen for winding. Three voltage taps over 5 cm, 10 cm and 65 cm around the edge are used for the I_c test.

Each measurement of the strand is characterized by both cable twist-pitch (5) and appropriate bending radius (4). In the measurements with twist-pitches higher than 1.0 m, i.e.

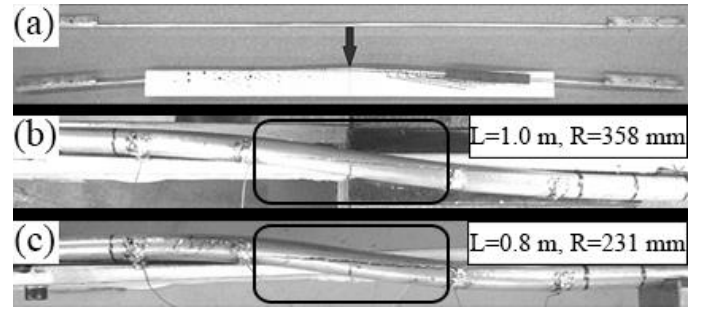


Fig. 10. (a) Strand winding on the aluminum core; (b) Strand without cracks; (c) Strand with cracks.

bending radii higher than 358 mm, the strand successfully withstands mechanical loads, Fig. 10 (b). In the last test with $L = 0.8$ m, $R = 231$ mm cracks between profiles are observed, Fig. 10 (c), in agreement with results of the previous bending test of the “normal” sample and confirms the set of equations, which were used for the cable design. The results of the strand’s critical current are presented in Fig. 11.

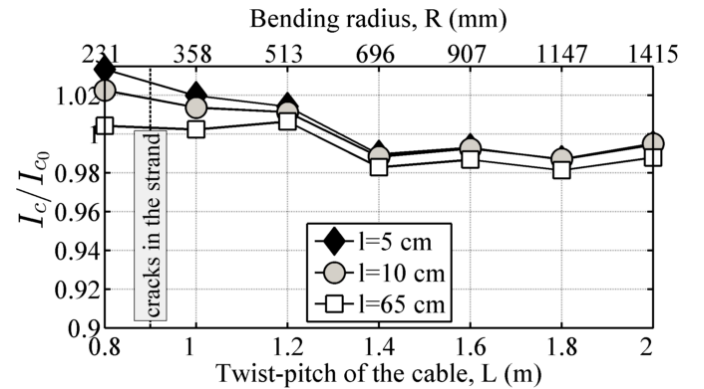


Fig. 11. Critical current of the strand as a function of the cable twist-pitch.

The cracks in the strand occur earlier than noticeable degradation of the critical current. Even slightly opposite effect takes place: in the place with opened profiles the stack of tapes gets a bit more “freedom” in the position, which allows partial strain relaxation. Nevertheless, according to the bending properties of the “normal” strand (see Table I and Fig. 4), degradation of critical current starts soon after the cracks origin.

V. CONCLUSION

The preliminary annealing of the strand’s copper profile greatly improves the bending properties of the strand. The critical bending radius shifted from the initial value of 500 mm to 240 mm. The proposed analytical model of the strand’s bending, validated by the test results, could be implemented in further analysis of the strand with new parameters.

A set of the parameters for cored Rutherford cable with CRPP strands is obtained, verified and will be used for the full size prototype.

ACKNOWLEDGMENT

The authors thank the Paul Scherrer Institute (PSI) for the technical support.

REFERENCES

- [1] D. Uglietti, R. Wesche, and P. Bruzzone, "Design and strand tests of a fusion cable composed of coated conductor tapes," *IEEE Trans. Appl. Supercond.*, vol. 24, no. 3, 4800704, Jun. 2013.
- [2] M. Takayasu, L. Chiesa, L. Bromberg and J. V. Minervini, "HTS twisted stacked-tape cable conductor," *Supercond. Sci. Technol.*, vol. 25, no. 1, 014011, Dec. 2012.
- [3] N. Bykovsky, S. Fetisov, A. Nosov, V. Zubko, and V. Vysotsky, "Analysis of critical current reduction in self-field in stacked twisted 2G HTS tapes," *Journal of Physics Conference Series* 022001, May 2014
- [4] S. P. Timoshenko and J. N. Goodier, *Theory of Elasticity*, 3rd ed.: McGraw-Hill Book Company, 1970.
- [5] P. Sunwong, J. S. Higgins, Y. Tsui, M. J. Raine and D. P. Hampshire, "The critical current density of grain boundary channels in polycrystalline HTS and LTS superconductors in magnetic fields," *Supercond. Sci. Technol.*, vol. 26, no. 9, 095006, Sep. 2013.
- [6] M. Takayasu, F. J. Mangiarotti, L. Chiesa, L. Bromberg, and J.V. Minervini, "Conductor characterization of YBCO twisted stacked-tape cables," *IEEE Trans. Appl. Supercond.*, vol. 23, no. 3, p. 4 800 104, Jun. 2013.
- [7] M. N. Wilson, "Superconductivity and accelerators: the good companions," *IEEE Trans. Appl. Supercond.*, vol. 9, no. 2, pp. 111 – 121, Jun. 1999.
- [8] P. K. Rashevsky, *A Course in Differential Geometry*, 3rd ed.: GITTL [in Russian], 1950.
- [9] R. Wesche, P. Bruzzone, D. Uglietti, N. Bykovsky, "Upgrade of SULTAN / EDIPO for HTS Cable Test," submitted for publication.